







## Open Archive Toulouse Archive Ouverte (OATAO)

OATAO is an open access repository that collects the work of Toulouse researchers and makes it freely available over the web where possible

This is an author's version published in: <http://oatao.univ-toulouse.fr/23777>

**Official URL:** <https://doi.org/10.1016/j.ceramint.2019.02.048>

### To cite this version:

Radingoana, Precious Manti  and Guillemet, Sophie  and Olubambi, Peter A. and Chevallier, Geoffroy  and Estournès, Claude  *Influence of processing parameters on the densification and the microstructure of pure zinc oxide ceramics prepared by spark plasma sintering.* (2019) *Ceramics International*, 45 (8). 10035-10043. ISSN 0272-8842

Any correspondence concerning this service should be sent to the repository administrator: [tech-oatao@listes-diff.inp-toulouse.fr](mailto:tech-oatao@listes-diff.inp-toulouse.fr)

# Influence of processing parameters on the densification and the microstructure of pure zinc oxide ceramics prepared by spark plasma sintering

P.M. Radingoana<sup>a</sup>, S. Guillemet-Fritsch<sup>a,\*</sup>, P.A. Olubambi<sup>b</sup>, G. Chevallier<sup>a</sup>, C. Estournès<sup>a</sup>

<sup>a</sup> CIRIMAT, Université de Toulouse, CNRS, Université Toulouse 3 - Paul Sabatier, 118 Route de Narbonne, 31062, Toulouse cedex 9, France

<sup>b</sup> University of Johannesburg, School of Mining, Metallurgy and Chemical Engineering, Johannesburg, South Africa

## ARTICLE INFO

### Keywords:

ZnO  
Spark plasma sintering  
Nanoparticles  
Ceramics  
Microstructure

## ABSTRACT

Due to the sensitivity of nanopowders and the challenges in controlling the grain size and the density during the sintering of ceramics, a systematic study was proposed to evaluate the densification and the microstructure of ZnO ceramics using spark plasma sintering technique. Commercially available ZnO powder was dried and sintered at various parameters (temperature (400–900 °C), pressure (250–850 MPa), atmosphere (Air/Vacuum) etc.). High pressure sintering is desirable for maintaining the nanostructure, though it brings a difficulty in obtaining a fully dense ceramic. Whereas, increasing the temperature from 600 to 900 °C results in fully densified ceramics of about 99% which shows to have big impact on the grain size. However, a high relative density of 92% is obtained at a temperature as low as 400 °C under a pressure of 850 MPa. The application of pressure during the holding time seems to lower the grain size as compared to ceramics pressed during initial stage (room temperature).

## 1. Introduction

For several decades, zinc oxide (ZnO) has been broadly investigated in electronics (thermoelectricity, gas sensing, piezoelectric, optoelectronics etc.) and laser technology because of its unique properties [1–6]. It has wide broad energy band (3.37 eV), high bond energy, and high thermal, chemical and mechanical stability. Being a non-toxic and abundant material, it is mostly used in many applications as an initiative towards green technology. Recently, the use of ZnO nanoparticles has been mostly preferred in modern electroceramic applications, because of their large surface areas, unusual adsorptive properties, surface defects and fast diffusivities [7]. As a result, the sintering temperature could be lowered and the properties of materials improved. For instance, there have been reports about sintering of ZnO nanoparticles at low temperatures, less than 600 °C [8–11]. This causes less grain growth which is beneficial for enhancing photocatalytic activity, nonlinear current-voltage characteristics and thermoelectric properties.

To obtain optimal properties of ZnO nanoparticles and enhance their applications, it is important to have better control of their crystallinity, particle size and morphology. Since 1990s, there has been an interest in producing specific nanoparticles with unique nanostructure.

Their efficiency and specific application highly depend on the particle size distribution and grain morphology of the materials. Various investigations have been focused on understanding relevant factors and optimizing the processing parameters for large scale application of ZnO powders. Nanopowder synthesis methods such as hydrothermal and chemical precipitation have been used to prepare ZnO nanoparticles. Since hydrothermal technique is energy intensive, most studies have been focussed on chemical precipitation method as it is cost efficient.

One of the most crucial issues with consolidating ceramic nanopowders is obtaining full densification. Extensive studies have been done on the conventional sintering (such as hot pressing, pressureless sintering and hot isostatic sintering [12,13]) of nanopowder materials. Relative density of above 95% is reached at high temperature (800–1200 °C) and long sintering periods (> 2 h) when using these techniques, which causes grain growth due to diffusion of grain boundaries and Ostwald ripening [14–18]. Much work is currently being focused on finding ways to minimize grain growth and improve ceramic properties.

Spark plasma sintering (SPS) is a recent effective sintering technique for consolidating all kinds of materials [19]. It uses rapid heating and high thermal efficiency, and as a result, it contributes to full densification of materials within minutes with retained nano-

\* Corresponding author.

E-mail address: [guillem@chimie.ups-tlse.fr](mailto:guillem@chimie.ups-tlse.fr) (S. Guillemet-Fritsch).

microstructure [13,20–23]. Despite the effectiveness of SPS technology, only few publications are available on SPS of pure ZnO.

Aimable et al. [14] reported that synthesized powder could not be densified by traditional methods, though using SPS they could densify to 99.5% with grain size of  $0.2 \pm 0.8 \mu\text{m}$  at  $900^\circ\text{C}$ . Whereas, commercial powder could only be densified to 95.1% with grain size of  $1 \pm 0.5 \mu\text{m}$  using similar SPS conditions. A fully dense ceramic of 98% was obtained when using conventional sintering at  $1100^\circ\text{C}$  for 4 h. This indicates the influence of powder quality on the sintering mechanism of ZnO ceramics. It is also evident that the rapid heating of SPS allows lower sintering temperatures during a short period of time. Schwarz et al. [11] were able to densify nanocrystalline ZnO up to relative density (RD) of 95% at low temperature of  $400^\circ\text{C}$ . They also indicated that heating rates affects the sintering behaviour of nano ZnO ceramics, the higher the heating rate the better the densification kinetics during heating ramp and holding time. However, the recent reports by Virtudazo et al. [24] on sintering of nanoporous ZnO stressed about the influence of powder morphology on the sintering mechanism. The ceramics were only densified to 78–91% when sintering was performed between  $550$  and  $950^\circ\text{C}$ . Sintering above  $750^\circ\text{C}$  resulted ceramic grain sizes of about  $10 \mu\text{m}$  due to high surface area of the starting powder. Zhang et al. [25] sintered micro nanostructured (hybrid) powders using SPS in which they got less dense ceramic of 84% at  $900^\circ\text{C}$ .

Recent work [9,11,26,27] focuses on the SPS sintering of ZnO nanoparticles at low temperatures (less than  $400^\circ\text{C}$ ) by adding solvents (such as water, aqueous acetic acid, etc. ...) to enhance densification. Dargatz et al. [9,26] were able to get a fully dense ZnO ceramic at  $400^\circ\text{C}$  by controlling the heating rates, water content and electric field. About 99.9% relative density was reported when using 1.6 wt% water, however, isotropic structures were observed due to diffusion of hydrogen and hydroxide ions into the ZnO crystallite. The improved densification at such low temperatures is due to the adsorbed water on the surface of the ZnO particles that reduces the inter particles friction allowing better mobility of the particles and dissolution of  $\text{Zn}^{2+}$  and  $\text{O}^{2-}$  ions on the grain's surface during sintering. Gonzalez Julian et al. [27] recently reported the lowest sintering temperature of  $250^\circ\text{C}$ ; densification of 97.3% was obtained using aqueous acetic acid.

Even though highly densified ZnO has been reported at low temperature using sintering aids, it is important to have better understanding on the sintering behaviour of dry and/or undoped ZnO ceramics. The few reports mostly focus on the effect of sintering temperature on the sintering behaviour of newly synthesized powders. In this work, a commercially available ZnO powder was used to perform a systematic study on the densification characteristics and the microstructure of ZnO ceramics using spark plasma sintering technique. The influence of parameters such as temperature, pressure, current insulation, sintering atmosphere and period of pressure application were fully evaluated.

## 2. Experimental method and procedure

### 2.1. Preparation and characterization of powder

Commercially available zinc oxide (ZnO) (Sigma Aldrich) of high purity (99.99%) and submicronic particle size was used in this study. The powder was dried at  $150^\circ\text{C}$  overnight before sintering to ensure no adsorbed moisture. After drying, the powder was ambient cooled and sealed with a moisture resistant plastic (Parafilm Moisture Proof Sealing) before sintering. To identify any organic structures in the powders Fourier Transform Infrared Spectroscopy (FTIR) (Spectrometry Frontier and Microscope Spotlight 400 Series: MIR NIR) was used. Recordings were done at a wavelength range of  $650$ – $4000 \text{ cm}^{-1}$ . The thermal behaviour of the powder was studied using Differential Thermal Analysis (DTA) and thermogravimetric analysis (DTG) (Setaram TAG16) at a heating rate of  $3^\circ\text{C}/\text{min}$  up to  $1000^\circ\text{C}$ . The ZnO powder was analysed by X ray diffractometer (XRD Bruker D4). The diffraction patterns were recorded using copper cathode as radiation source ( $K\alpha$ , wavelength  $1.5418\text{\AA}$ ) in the range  $10$ – $80^\circ$  with an acquisition step of  $0.01^\circ$ . Brunauer Emmett Teller technique (BET) (Micromeritics desorb 2300A) was used to determine the surface area. The grain sizes were estimated from the surface area (BET) using Eq. (01) [28]. This method assumes that the grains are spherical without any pores.

$$d_{\text{BET}} = \frac{6}{\rho \times S_{\text{BET}}} \quad (1)$$

Where  $d_{\text{BET}}$  is the crystallite size (m),  $\rho$  is the density of the sample ( $\text{g}/\text{m}^3$ ) and  $S_{\text{BET}}$  is the surface area ( $\text{m}^2/\text{g}$ ). Powder morphology was studied by Scanning Electron Microscopy (MEB JEOL JSM65 10LV). Chemical composition of the powders was obtained by inductively coupled plasma atomic emission spectroscopy (ICP AES).

### 2.2. Densification of ZnO by spark plasma sintering (SPS)

The commercial ZnO powder was densified with a Dr. Sinter 2080 unit (SPS Syntex Inc., Japan) available at the Plateforme Nationale de Frittage Flash (PNF2) located at the Université Toulouse 3 Paul Sabatier using 8 and 20 mm inner diameter tungsten carbide and graphite dies. The molds were lined with 0.2 mm thick graphite foil (PERMA FOIL®Toyo Tanso). Several parameters were varied during the study with the aim to get fully dense pellets with minimal grain growth. Sintering pressure (250–850 MPa), temperature ( $400$ – $700^\circ\text{C}$ ), atmosphere (Air and Vacuum), current insulation and sintering cycle were investigated.

The sintering cycles (SC) which were compared in this study are shown in Fig. 1. Sintering cycle 1 (SC1) reported in Fig. 1 (a; b) was used for all the test work. The cycle in Fig. 1 (a) was used for 8 mm samples. Uniaxial pressure was applied at room temperature for 2 min followed by temperature increase at a ramp up speed of  $100^\circ\text{C}/\text{min}$ . The isothermal time was kept for 6 min. The temperature was cooled at a rate of  $100^\circ\text{C}/\text{min}$  simultaneously with pressure release. For the 20 mm

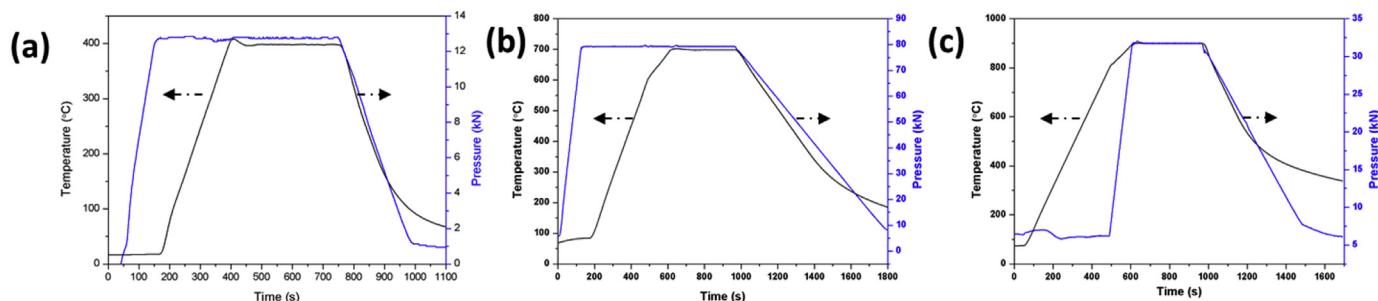


Fig. 1. SPS sintering cycles: (a) SC1 for 8 mm die (b) SC1 for 20 mm and (C) SC2.

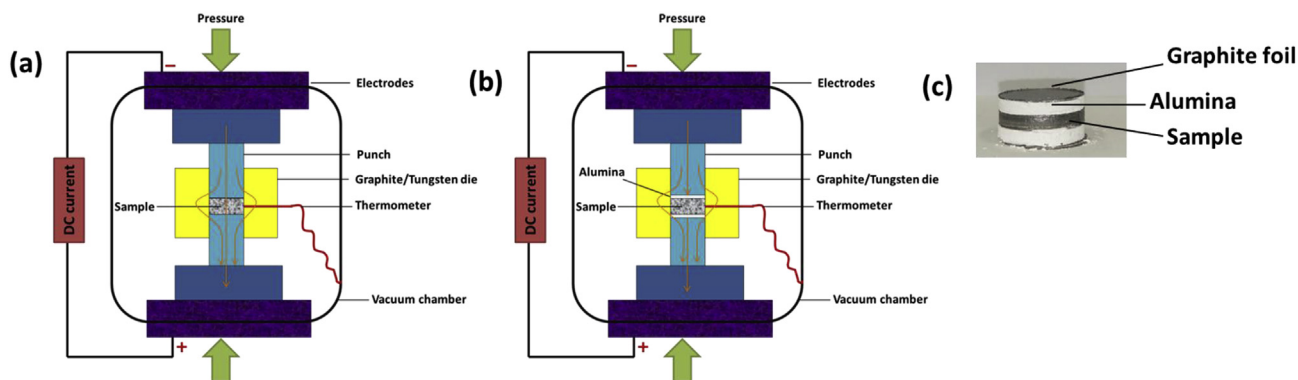


Fig. 2. Scheme of the SPS column: (a) Un-insulated setup (b) Current isolation using alumina (c) Sample preparation with alumina.

samples the heating rate was reduced to 50 °C/min when it approached the dwell time to avoid temperature overshoot. The other sintering cycle (SC2) entails applying the temperature first and followed by application of axial pressure for 2 min towards the dwell time.

A schematic diagram of SPS column is illustrated in Fig. 2. It shows the flow of current for “un insulated” setup (Fig. 2 (a)) and “current insulated” using alumina (Fig. 2 (b)). About 2 g of alumina powder was put on both sides of a sample as shown in Fig. 2 (c). Misawa et al. [29] and Yang et al. [30] reported on the influence of internal current on pure ZnO and ZnO/Al ceramics during sintering, respectively. It was found that the progress of sintering changes based on whether current passes through sample or not. Insulation prevents the influences of electric field on the ZnO grains; which affects the reactivity and diffusion during sintering.

### 2.3. Characterization of ZnO ceramics

The ZnO ceramics were polished by silicon carbide discs (P320 and P600) to remove graphite foil. The density of the ceramics was measured by Archimedes method and the relative density was calculated taking the theoretical density as 5.681 g/cm<sup>3</sup>. For pellets with relative density of < 92%, geometric density was calculated. XRD and SEM analysis were conducted to confirm phase composition and microstructure. The ceramics were not annealed after sintering.

## 3. Results and discussion

### 3.1. Characterization of the commercial ZnO powder

SEM analysis of the commercial ZnO powder evidenced irregular morphology of the grains (Fig. 3 (a)). The grains have elongated and spherical structures due to the low surface energy associated with high polar plane (002). The particle size distribution of the powder is given

in Fig. 3 (b), it showed that majority of the grain sizes ranges between 100 and 250 nm. A mean grain size of 193 nm was determined with a surface area of 5.8 m<sup>2</sup>/g. The XRD analyses indicated that the powder has characteristic signature of zinc oxide hexagonal wurzite structure (ICPSD No. 01 070 8070, Fig. 4). The elemental analysis showed that powder has low concentration of impurities (Al, Mg, K, Ta, S, and P), less than 5 ppm. FTIR analyses indicated reduced concentration of nitrates (NO<sub>2</sub>) and hydroxides (O–H) by roughly 85% after drying. The total mass loss of the dried powder reduced from 0.49% to 0.26% when heated upto 1000 °C, probably indicating decomposition and/or of moisture and nitrates in the powder.

### 3.2. Spark plasma sintering of ZnO ceramics

Spark plasma sintering (SPS) of pure ZnO ceramics was explored with the aim to get fully dense pellets and fine microstructure. The effect of SPS parameters on the relative density and microstructure of ZnO ceramics was extensively explored. The parameters which were varied are: pressure, temperature, sintering atmosphere, current isolation, period of pressure application and die geometry. The summary of the relative density and grain size of the different samples are given in Table 1.

#### 3.2.1. Effect of sintering pressure

The effect of sintering pressure on the microstructure and densification of zinc oxide ceramics was investigated using an 8 mm tungsten carbide die. The pressure was varied between 250 and 850 MPa at a fixed temperature of 400 °C. It was observed that the relative density gradually increases from 77% to 92% as the sintering pressure is increased from 250 to 850 MPa (Fig. 5). The improved densification is due to the re arrangement of the particles by rotation [21]. Dargatz et al. [9,26] previously reported on the sintering of pure ZnO at 400 °C and 50 MPa in a dry and wet state. Relative densities of 59% and 100%

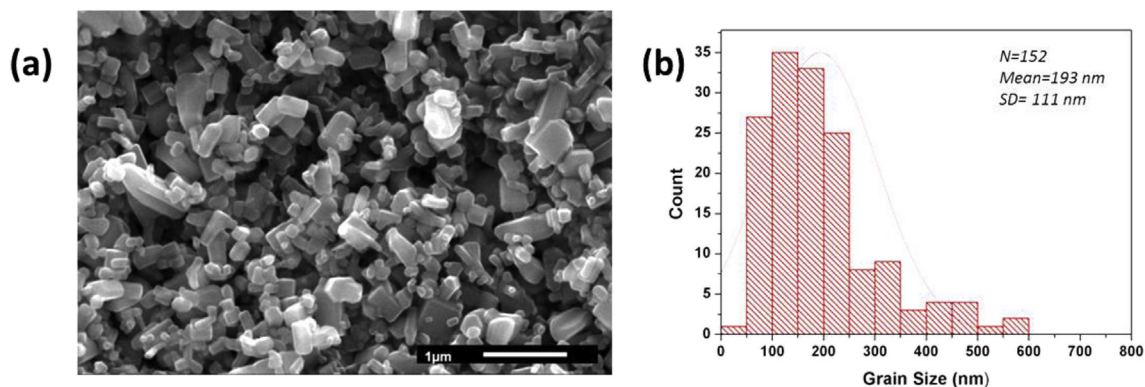


Fig. 3. SEM micrograph (a) of commercial zinc oxide powder and corresponding particle size distribution (b).

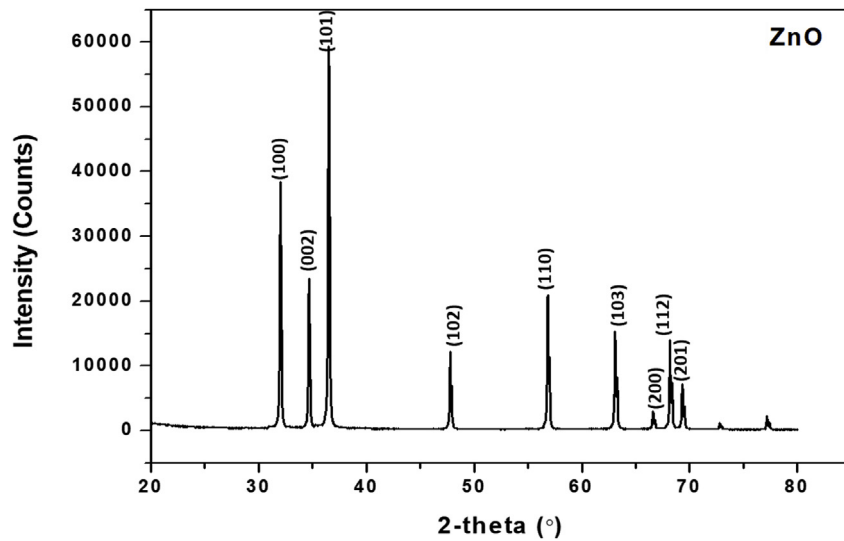


Fig. 4. XRD patterns of zinc oxide powder.

were reported for dry and wet state (1.6 wt% water), respectively. To our knowledge, this is the first report on high relative density of 92% obtained for pure ZnO in a dry state sintered at 850 MPa at temperature as low as 400 °C.

The dense ceramics were analysed by XRD to confirm the phase structure. The XRD patterns of the sintered ZnO ceramics are similar to that of as received powder, i.e. the wurzite structure. No phase change occurs during sintering within the range of pressure used in this work.

The fracture surface of the samples sintered at various pressures was analysed by SEM (Fig. 6). Grain sizes determined through image J are given in Fig. 5. It was observed that at lower pressure of 250 MPa the grain growth is more obvious compared to pressures above 350 MPa. The grains looked more defined. Increasing the sintering pressure up to 850 MPa does not cause much grain growth as quantified by the mean grain sizes (~220 nm) in Fig. 5. A review by Chaim et al. [21] reported on the similar behaviour from cubic zirconia [31] and magnesium aluminate spinel [32,33]. The increase in the pressure affects the pore

closure during densification. It is the first time reporting on the effect of pressure on pure ZnO sintered by spark plasma sintering technique. Some visible pores confirm that the ceramics are not fully dense.

### 3.2.2. Effect of sintering temperature

The effect of sintering temperature on the densification of ZnO ceramics was carried out under air atmosphere. This study was performed using a 20 mm tungsten carbide die. A sintering pressure of 250 MPa was used to avoid deformation of tungsten carbide die at high temperatures. The relative density is shown in Fig. 7, as a function of the sintering temperature. With an increase in sintering temperature the relative density of the ceramics was improved up to  $99 \pm 0.4\%$  at temperature as low as 600 °C. Between 600 °C and 700 °C the relative density did not seem to change much (~99%). Gao et al. [34] reported a decrease in the relative density of pure ZnO ceramics from 98.5% to 97% when sintering between 550 °C and 700 °C in vacuum was observed. This could have been caused by the creation of pores due to

Table 1

Relative density and grain size of ceramics prepared from commercial ZnO powder for different sintering conditions [*Symbols: SC is sintering cycle and RT is room temperature*].

Study	Die diameter	Atmosphere	Sintering cycle	Insulation	Temperature	Pressure & when applied	Relative density	3D grain size (Image J)
-	mm	-	-	-	°C	MPa	%	µm
Pressure	8	Air	SCI	Without	400	250.RT	$76,5 \pm 2,2$	$0,38 = 5 = 0,13$
	8	Air	SCI	Without	400	350.RT	$76,9 = 0,7$	$0,36 = 5 = 0,13$
	8	Air	SCI	Without	400	450.RT	$85,2 \pm 1,2$	$0,29 \pm 0,13$
	8	Air	SCI	Without	400	550.RT	$85 \pm 1,7$	$0,27 \pm = 0,13$
	8	Air	SCI	Without	400	700.RT	$89,7 = 1,4$	$0,24 \pm 0,13$
	8	Air	SCI	Without	400	850.RT	$92,2 = 1,2$	$0,22 \pm 0,13$
Temperature	20	Air	SCI	Without	25	250.RT	64.4	$0,20 \pm 0,13$
	20	Air	SCI	Without	400	250.RT	$76,5 \pm 2,2$	$0,4 \pm 0,1$
	20	Air	SCI	Without	500	250.RT	$95,3 = 0,1$	$0,5 \pm 0,1$
	20	Air	SCI	Without	600	250.RT	$99,4 = 0,4$	$3,3 \pm 1,5$
	20	Air	SCI	Without	700	250.RT	$99,1 \pm 0,5$	$5,4 \pm 2,1$
Die geometry dimensions Sintering atmosphere	8	Air	SCI	Without	700	250.RT	$97,8 = 1,2$	$5,3 \pm 2,3$
	20	Vacuum	SCI	Without	700	250.RT	$98,8 = ,9$	$4,3 \pm 1,9$
	20	Vacuum	SCI	Without	900	100.RT	$97,8 = 0,5$	$10,3 = 3,6$
Current isolation Application of pressure	20	Vacuum	SCI	With	900	100.RT	$98,0 = 1,3$	$5,1 \pm 1,8$
	20	Vacuum	SC2	With	900	100. Last 2 min of heating stage	$98,7 = 0,4$	$3,6 \pm 1,3$



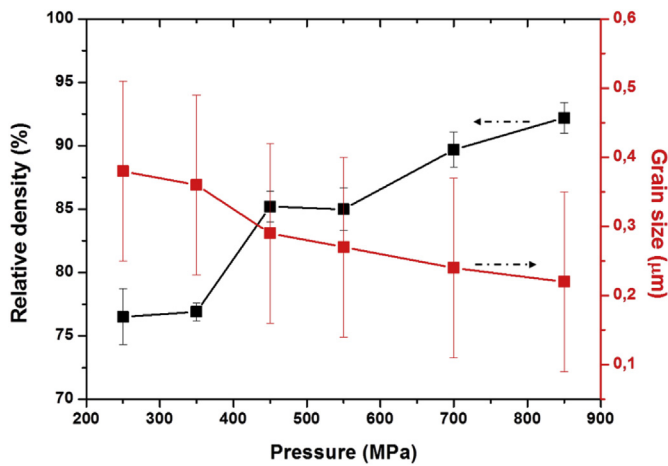


Fig. 5. Relative density and grain size as a function of pressure for ceramics prepared from commercial ZnO powder ( $T = 400\text{ }^{\circ}\text{C}$ ).

grain growth [35]. The rate of grain growth relies on the initial powder quality (grain size, porosity); a powder with high specific area would result fast reaction rates. Hence, it is vital to be cautious about preparation methods of starting powders.

The fracture surface micrographs of the ceramics obtained at various temperatures are given in Fig. 8. The corresponding grain sizes are given in Fig. 7, which were determined by analysis of SEM micrographs (Image J on  $\sim 27$  particles). There is an increase in the grain size from initial size of 193 nm to  $5.5 \pm 2.2\text{ }\mu\text{m}$ , when sintering is performed at  $700\text{ }^{\circ}\text{C}$ , 250 MPa. According to Aimable et al. [14] such grain growth is controlled by the diffusion rate of zinc ions within the crystal structure [14]. Hence, the neighbouring grains diffuse into each other at the grain boundaries causing grain growth during sintering [36]. It is also shown that the grains become more defined and sharper at  $600\text{ }^{\circ}\text{C}$  and  $700\text{ }^{\circ}\text{C}$  (Fig. 8).

The pictures of the as sintered ZnO ceramics are given in Fig. 8. It was noticed that there is a colour change from the initial starting white powder. The ceramics becomes yellow at  $500\text{ }^{\circ}\text{C}$ , grey at  $600\text{ }^{\circ}\text{C}$  and grey whitish at  $700\text{ }^{\circ}\text{C}$ . The phase structure of the as sintered is similar to the one of the raw powder. The structure is the wurzite crystal. Han [37] attributed the colour change to oxygen deficiency in dually doped ZnO composites (Al, Cd, Ga, Sc). In the present case, the colour change is due to oxygen deficiency related to the low partial pressure of oxygen at high temperatures.

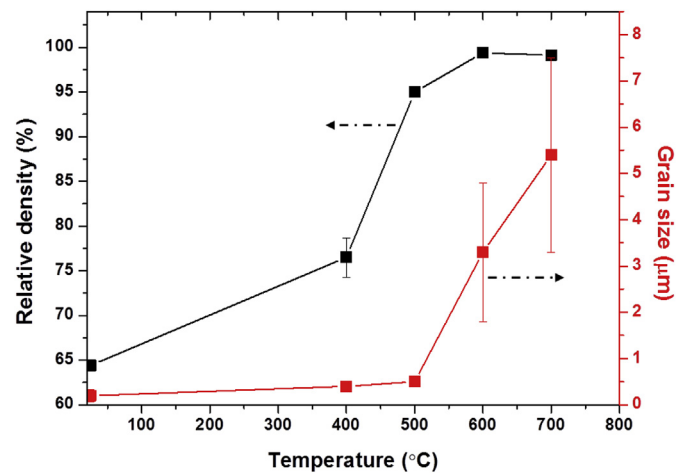


Fig. 7. Relative density and grain size of ceramics prepared from commercial ZnO as a function of temperature ( $P = 250\text{ MPa}$ ).

### 3.2.3. Influence of die diameter

Two tungsten carbide dies presenting different inner diameters (8 mm and 20 mm) were used in order to see if a change in dimensions could affect the microstructure and relative density of ceramics prepared from commercial powder. Sintering at  $700\text{ }^{\circ}\text{C}$  and 250 MPa (air atmosphere) was chosen to ensure full densification of ZnO ceramics due to the changes in temperature distribution when a different die size is used. The relative density is 97.8% and 99.1% for 8 and 20 mm die diameter, respectively. The SEM micrographs in Fig. 9 indicated that the grain size distribution for 8 and 20 mm ceramics looks similar (Fig. 9 (b)). This implies that temperature distribution of the two dies does not vary much when sintering ZnO ceramics. However, electro thermal simulations on alumina sample by finite element modelling on 10 and 20 mm inner diameter graphite dies have shown, a difference of about  $100\text{ }^{\circ}\text{C}$  for the same setpoint fixed at the surface of the tool [38]. Thus, densification characteristics rely on the sintered material, type and diameter of die. In this study, the change of die diameter from 8 to 20 mm does not significantly influences the densification of pure ZnO.

### 3.2.4. Influence of sintering atmosphere

The influence of sintering atmosphere on the relative density and grain size of ZnO ceramics was studied using 20 mm die. Since ZnO is easily reduced, the oxygen partial pressure plays a huge role on the densification of ZnO ceramics. Two different sintering atmospheres: air and vacuum were used to sinter commercial ZnO powder. These will allow changing the oxygen stoichiometry of ZnO ceramics and to

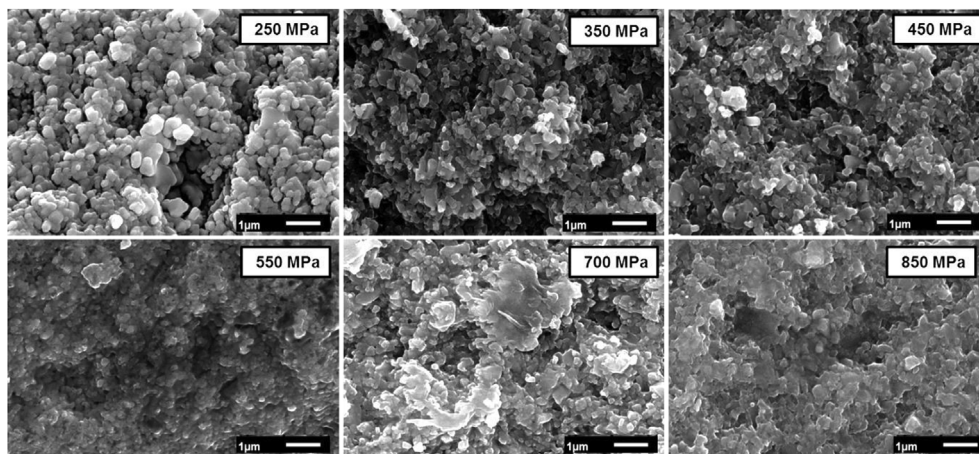


Fig. 6. SEM micrograph of fractured surface of ceramics prepared from commercial ZnO powder at various pressures ( $T = 400\text{ }^{\circ}\text{C}$ ).

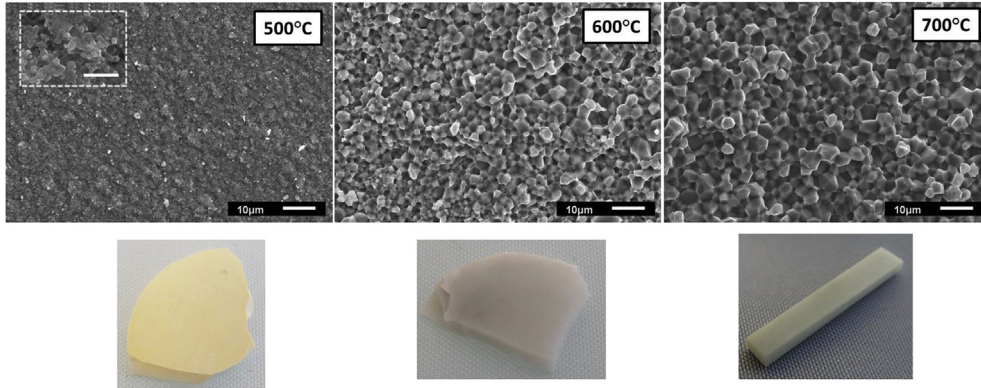


Fig. 8. SEM micrographs of fractured surfaces and pictures of as-sintered ceramics showing the effect of sintering temperature.

evaluate its effects on the morphology and relative density. The summary of the samples characteristics for different atmospheres are given in Table 1. A relative density of 98.7% and 98.8% is obtained when operating in air and vacuum; respectively (700°C and 250 MPa). The SEM micrographs are given in Fig. 10; there is only a small difference of roughly 1.7 µm between the grain sizes of the ceramics (Fig. 10 (b)). Hence, the morphology and relative density are not affected when the sintering is performed in air or vacuum at 700°C and 250 MPa.

For further comparison, the temperature was increased to 900°C in order to make a more oxygen deficient ceramic. In oxygen deficient environment, the first stages of densification of ZnO is controlled by the diffusion of oxygen atoms which can be easily influenced by the external oxygen partial pressure [39,40]. In that manner, more zinc interstitials are created as shown in the general reduction oxidation reaction:



The relative density slightly decreased to 97.8% when the temperature was increased to 900 °C. Previous studies on the conventional sintering of pure ZnO ceramics indicated that higher densification was obtained in oxygen rich atmosphere than in air [17,41]. Thus, sintering occurs by means of oxidation of the excess zinc ions. The SEM micrograph is given in Fig. 11 (un insulated: 900°C); the grain size increases as the temperature increases: from 5.3 µm (700°C) to 10.3 µm (900°C). The inserted image showed that there are pores in the ceramic sintered at 900 °C which could have been caused by grain growth [35]. This justifies the decrease in the relative density. It was also observed that the grains have some pits on them which could be due to the evaporation of ZnO above 900 °C.

### 3.2.5. Influence of current isolation

The effect of current on ZnO ceramics was investigated for sintering treatment performed at 900 °C in vacuum. The relative density of pure ZnO ceramics with and without current is given in Table 1. Whatever

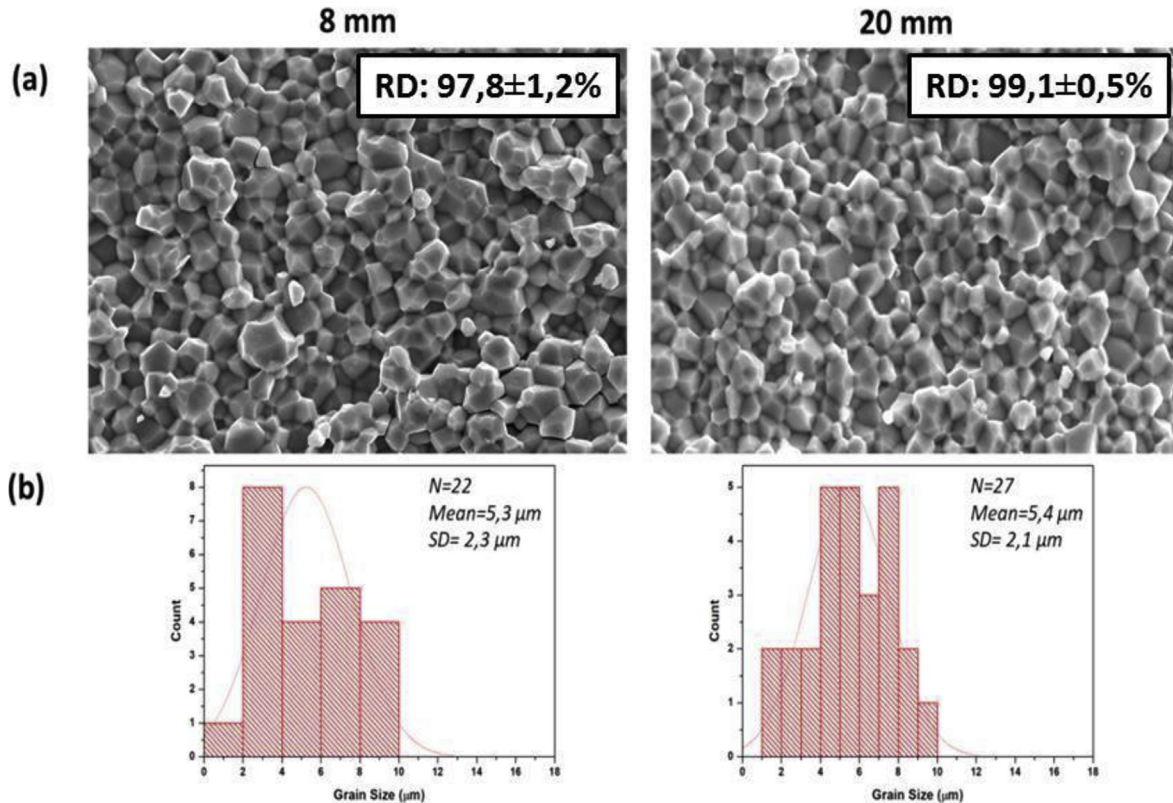


Fig. 9. (a) SEM micrograph of fractured surfaces (b) grain size distribution of ceramics prepared from commercial ZnO powder for 8 mm and 20 mm die.



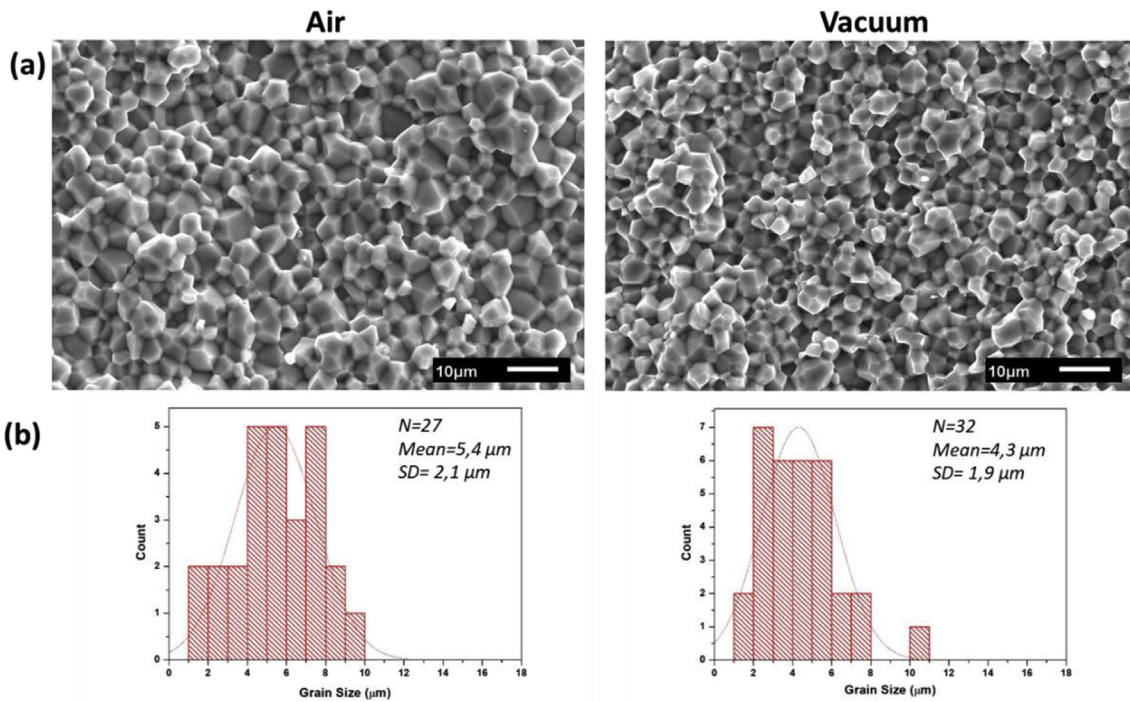


Fig. 10. (a) SEM micrograph of fractured surfaces (b) grain size distribution (Image J) of ceramics prepared from ZnO powder (700 °C 250 MPa).

the current condition, the relative density does not change respectively 97.8% and 98%. The SEM micrographs are given in Fig. 11 (un insulated: 900°C and Insulated: 900°C). There is a decrease in the grain size when the sintering is done without current passing through the sample: contrary to the average value of 10.3 μm for the “un insulated cycle”. The grain growth in the normal setup could have been contributed by Joule heating [29]. While for insulated one the densification took place by heat radiation from the die surface. Retainment in the microstructure with visible grain boundaries was previously reported on sintering pure ZnO ceramic with current isolation. While a ceramic sintered with current passing through did not show any grain boundaries i.e. neighbouring grains diffused into each other. This supports the observed results in this work.

### 3.2.6. Influence of period of pressure application

The effect of the period at which pressure is applied during sintering was investigated on the relative density and morphology of pure ZnO ceramics prepared from commercial powder. Two conditions were compared: pressure applied at room temperature (SC1) and the last 2 min of heating stage (SC2). The sample was sintered in vacuum with current isolation at a sintering temperature and pressure of 900°C and 100 MPa, respectively. The relative density of the ceramics is given in Table 1. The relative density slightly improved from 98% (SC1) to 99% (SC2). The slight improvement in densification is due to easier particle sliding or rotation when the pressure is applied at high temperature [21,42]. The SEM micrograph of the ZnO ceramics is given in Fig. 11. The grain size decreased when SC2 was used. Moreover, the grain size

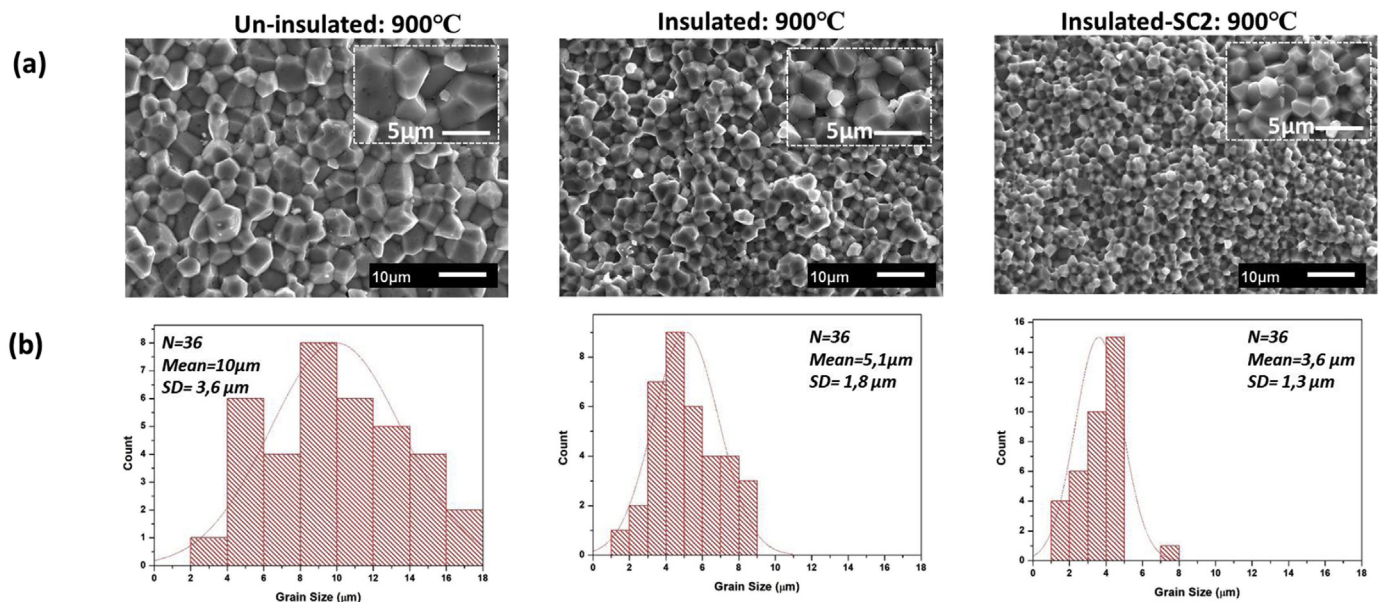


Fig. 11. (a) SEM micrograph of fractured surfaces (b) grain size distribution (Image J) of ceramics prepared from ZnO powder (900 °C 100 MPa).



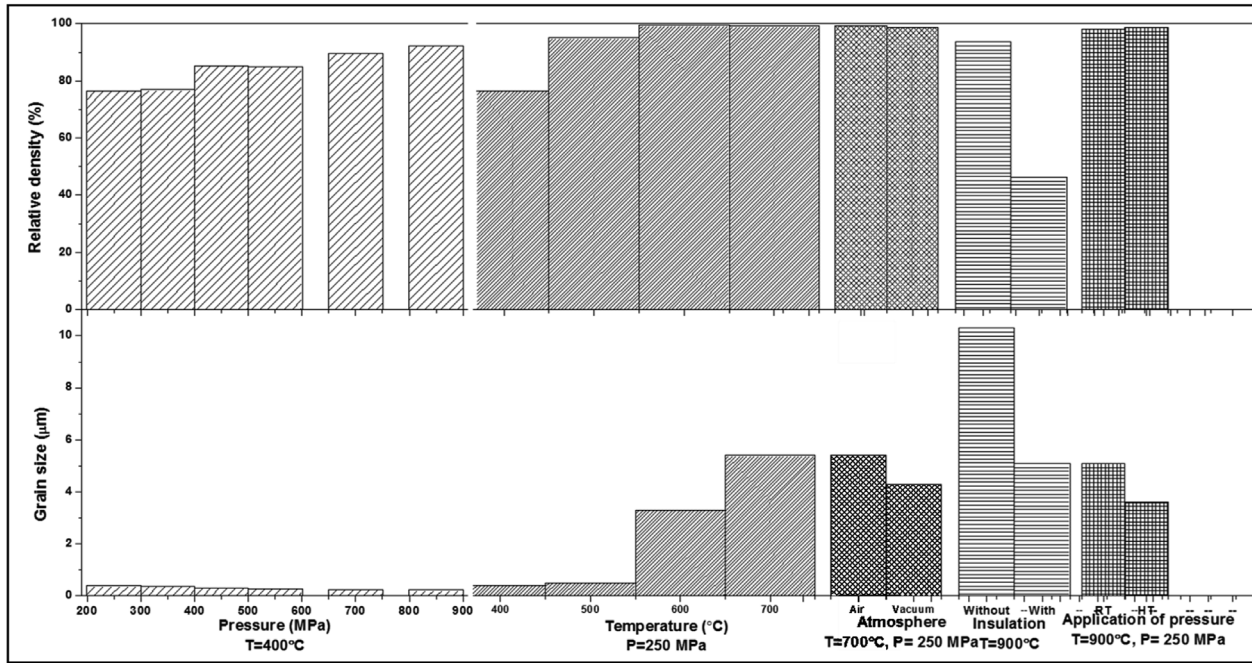


Fig. 12. Influence of SPS parameters on the densification and grain size of ZnO ceramics (Note: RT is room temperature and HT is holding temperature).

distribution is smaller. An average grain size of  $3.6\ \mu\text{m}$  was obtained which is lesser than SC1 by  $2.4\ \mu\text{m}$ . This could have been caused by the difference in heat transfer between the grains, SC1 had better contact as compared to SC2.

### 3.2.7. Summary of SPS parameters influence on pure ZnO ceramics

The overall view of the influence of SPS parameters on the relative density and grain size of pure ZnO ceramics is given in Fig. 12. High pressure sintering is desirable for maintaining the nanostructure, though the difficulty of obtaining a fully dense ceramic. Whereas, in creasing the temperature from 600 to  $900\ ^\circ\text{C}$  results in fully densified ceramics of about 99% which shows to have big impact on the grain size. Sintering of pure ZnO without insulation at  $900\ ^\circ\text{C}$  causes bigger grain sizes of about  $10\ \mu\text{m}$ . The application of pressure during the holding time seems to lower the grain size as compared to ceramics pressed during initial stage (RT). This figure could play as a guide to wards sintering of pure ZnO depending on the properties required for the final product.

## 4. Conclusions

The influence of processing parameters on the densification and the microstructure of pure zinc oxide ceramics prepared by spark plasma sintering was performed in this work. Increasing the pressure improves the relative density of ZnO ceramics due to particle rotation. A maximum relative density of 92% was obtained at a temperature as low as  $400\ ^\circ\text{C}$  for an applied pressure of 850 MPa. In this case the grain size is  $220 \pm 0.1\ \text{nm}$ . The increment of temperature up to  $600\ ^\circ\text{C}$  with a lower pressure, 250 MPa, lead to a significant increase of the relative density and grain size, respectively 99.4% and  $3.3\ \mu\text{m}$ .

The sintering atmospheres (air and vacuum) did not affect the densification and microstructure of ZnO ceramics. The impact of the electric current during sintering has been evaluated through experiments performed with or without insulation. There is no change in relative density but a grain size difference of  $7.8\ \mu\text{m}$  was obtained for the two conditions.

This study could provide a guide for controlling the densification and the grain size of ZnO ceramics obtained by spark plasma sintering of dried powders.

## Acknowledgements

This project was financially sponsored by A European and South African Partnership on Heritage and Past+ (AESOP+, Europe) and National Research Fund (NRF, South Africa).

## References

- [1] A. Janotti, C.G. Van de Walle, Fundamentals of zinc oxide as a semiconductor, Rep. Prog. Phys. (2009) 126501.
- [2] C.F. Klingshirn, A. Waag, A. Hoffmann, J. Geurts, Zinc Oxide: from Fundamental Properties towards Novel Applications, Springer Science & Business Media, 2010.
- [3] M. Willander, Q. Zhao, Q.-H. Hu, P. Klason, V. Kuzmin, S. Al-Hilli, et al., Fundamentals and properties of zinc oxide nanostructures: optical and sensing applications, Superlattice. Microsc. (2008) 352–361.
- [4] A. Moezzi, A.M. McDonagh, M.B. Cortie, Zinc oxide particles: synthesis, properties and applications, Chem. Eng. J. (2012) 1–22.
- [5] V. Krasil'nikov, T. Dyachkova, A. Tyutyunnik, O. Gyrdasova, M. Melkozerova, I. Baklanova, et al., Magnetic and optical properties as well as EPR studies of polycrystalline ZnO synthesized from different precursors, Mater. Res. Bull. (2018) 553–559.
- [6] T.K. Gupta, Application of zinc oxide varistors, J. Am. Ceram. Soc. (1990) 1817–1840.
- [7] M.S. El-Shall, D. Graiver, U. Pernisz, M. Baraton, Synthesis and characterization of nanoscale zinc oxide particles: I. laser vaporization/condensation technique, Nanostruct. Mater. (1995) 297–300.
- [8] Y. Beynet, A. Izoulet, S. Guillemet-Fritsch, G. Chevallier, V. Bley, T. Pérel, et al., ZnO-based varistors prepared by spark plasma sintering, J. Eur. Ceram. Soc. (2015) 1199–1208.
- [9] B. Dargatz, J. Gonzalez-Julian, M. Bram, P. Jakes, A. Besmehn, L. Schade, et al., FAST/SPS sintering of nanocrystalline zinc oxide—Part I: enhanced densification and formation of hydrogen-related defects in presence of adsorbed water, J. Eur. Ceram. Soc. (2016) 1207–1220.
- [10] O. Guillon, J. Gonzalez-Julian, B. Dargatz, T. Kessel, G. Schierning, J. Räthel, et al., Field-assisted sintering technology/spark plasma sintering: mechanisms, materials, and technology developments, Adv. Eng. Mater. 16 (2014) 830–849.
- [11] S. Schwarz, A.M. Thron, J. Rufner, K. Benthem, O. Guillon, Low temperature sintering of nanocrystalline zinc oxide: effect of heating rate achieved by field assisted sintering/spark plasma sintering, J. Am. Ceram. Soc. (2012) 2451–2457.
- [12] J. Langer, D.V. Quach, J.R. Groza, O. Guillon, A comparison between FAST and SPS apparatuses based on the sintering of oxide ceramics, Int. J. Appl. Ceram. Technol. (2011) 1459–1467.
- [13] R. Chaim, M. Levin, A. Shlayer, C. Estournès, Sintering and densification of nanocrystalline ceramic oxide powders: a review, Adv. Appl. Ceram. (2008) 159–169.
- [14] A. Aimable, H. Goure Doubi, M. Stuer, Z. Zhao, P. Bowen, Synthesis and Sintering of ZnO Nanopowders, Technologies, 2017, p. 28.
- [15] T. Senda, R.C. Bradt, Grain growth in sintered ZnO and ZnO-Bi<sub>2</sub>O<sub>3</sub> ceramics, J. Am. Ceram. Soc. (1990) 106–114.

- [16] T.K. Gupta, R.L. Coble, Sintering of ZnO: I, densification and grain growth\*, *J. Am. Ceram. Soc.* (1968) 521–525 Blackwell Publishing Ltd.
- [17] V. Lee, G. Parravano, Sintering reactions of zinc oxide, *J. Appl. Phys.* (1959) 1735–1740.
- [18] M.N. Rahaman, *Sintering of Ceramics*, CRC Press, New York, 2008.
- [19] R. Orru, R. Licheri, A.M. Locci, A. Cincotti, G. Cao, Consolidation/synthesis of materials by electric current activated/assisted sintering, *Mater. Sci. Eng. R Rep.* (2009) 127–287.
- [20] R. Chaim, R. Marder, C. Estournès, Z. Shen, Densification and preservation of ceramic nanocrystalline character by spark plasma sintering, *Adv. Appl. Ceram.* (2012) 280–285.
- [21] R. Chaim, G. Chevallier, A. Weibel, C. Estournès, Grain growth during spark plasma and flash sintering of ceramic nanoparticles: a review, *J. Mater. Sci.* (2018) 3087–3105.
- [22] J.G. Noudem, D. Kenfau, S. Quetel-Weben, C.S. Sanmathi, R. Retoux, M. Gomina, Spark plasma sintering of n-type thermoelectric Ca<sub>0.95</sub>Sm<sub>0.05</sub>MnO<sub>3</sub>, *J. Am. Ceram. Soc.* (2011) 2608–2612.
- [23] D. Kenfau, G. Bonnefont, D. Chateigner, G. Fantozzi, M. Gomina, J.G. Noudem, Ca<sub>3</sub>Co<sub>4</sub>O<sub>9</sub> ceramics consolidated by SPS process: optimisation of mechanical and thermoelectric properties, *Mater. Res. Bull.* (2010) 1240–1249.
- [24] R.V.R. Virtudazo, Q. Guo, R. Wu, T. Takei, T. Mori, An alternative, faster and simpler method for the formation of hierarchically porous ZnO particles and their thermoelectric performance, *RSC Adv.* (2017) 31960–31968.
- [25] D.-B. Zhang, H.-Z. Li, B.-P. Zhang, D.-d Liang, M. Xia, Hybrid-structured ZnO thermoelectric materials with high carrier mobility and reduced thermal conductivity, *RSC Adv.* (2017) 10855–10864.
- [26] B. Dargatz, J. Gonzalez-Julian, M. Bram, Y. Shinoda, F. Wakai, O. Guillon, FAST/SPS sintering of nanocrystalline zinc oxide—Part II: abnormal grain growth, texture and grain anisotropy, *J. Eur. Ceram. Soc.* (2016) 1221–1232.
- [27] J. Gonzalez-Julian, K. Neuhaus, M. Bernemann, J.P. da Silva, A. Laptev, M. Bram, et al., Unveiling the mechanisms of cold sintering of ZnO at 250° C by varying applied stress and characterizing grain boundaries by Kelvin Probe Force Microscopy, *Acta Mater.* (2018) 116–128.
- [28] J.M. Zielinski, *I. Chemicals, Pharmaceutical Physical Characterization: Surface Area and Porosity*, Intertek, Manchester, 2013.
- [29] T. Misawa, N. Shikatani, Y. Kawakami, T. Enjoji, Y. Ohtsu, H. Fujita, Observation of internal pulsed current flow through the ZnO specimen in the spark plasma sintering method, *J. Mater. Sci.* (2009) 1641–1651.
- [30] S. Yang, F. Chen, Q. Shen, L. Zhang, Microstructure and electrical property of aluminum doped zinc oxide ceramics by isolating current under spark plasma sintering, *J. Eur. Ceram. Soc.* (2016) 1953–1959.
- [31] D.V. Quach, H. Avila-Paredes, S. Kim, M. Martin, Z.A. Munir, Pressure effects and grain growth kinetics in the consolidation of nanostructured fully stabilized zirconia by pulsed electric current sintering, *Acta Mater.* (2010) 5022–5030.
- [32] M. Sokol, M. Halabi, Y. Mordekovitz, S. Kalabukhov, S. Hayun, N. Frage, An inverse Hall-Petch relation in nanocrystalline MgAl<sub>2</sub>O<sub>4</sub> spinel consolidated by high pressure spark plasma sintering (HPSPS), *Scripta Mater.* (2017) 159–161.
- [33] M. Sokol, M. Halabi, S. Kalabukhov, N. Frage, Nano-structured MgAl<sub>2</sub>O<sub>4</sub> spinel consolidated by high pressure spark plasma sintering (HPSPS), *J. Eur. Ceram. Soc.* (2017) 755–762.
- [34] L. Gao, Q. Li, W. Luan, H. Kawaoka, T. Sekino, K. Niihara, Preparation and electric properties of dense nanocrystalline zinc oxide ceramics, *J. Am. Ceram. Soc.* (2002) 1016–1018.
- [35] R.M. German, *Sintering Theory and Practice*, (1996).
- [36] M. Tokita, Mechanism of spark plasma sintering, *Proceeding of NEDO International Symposium on Functionally Graded Materials: Japan, 1999*, p. 22.
- [37] L. Han, High Temperature Thermoelectric Properties of ZnO Based Materials: Department of Energy Conversion and Storage, Technical University of Denmark, 2014.
- [38] C. Manière, Spark plasma sintering: couplage entre les approches: modélisation, instrumentation et matériaux, Université Paul Sabatier-Toulouse III, 2015.
- [39] C. Lin, B. Wang, Z. Xu, H. Peng, Densification and electrical properties of zinc oxide varistors microwave-sintered under different oxygen partial pressures, *J. Electron. Mater.* (2012) 3119–3124.
- [40] Z. Chen, S. Yamamoto, M. Maekawa, A. Kawasuso, X. Yuan, T. Sekiguchi, Postgrowth annealing of defects in ZnO studied by positron annihilation, x-ray diffraction, Rutherford backscattering, cathodoluminescence, and Hall measurements, *J. Appl. Phys.* (2003) 4807–4812.
- [41] T. Gupta, R. Coble, Sintering of ZnO: I, Densification and grain growth, *J. Am. Ceram. Soc.* (1968) 521–525.
- [42] J.G. Santanach, A. Weibel, C. Estournès, Q. Yang, C. Laurent, A. Peigney, Spark plasma sintering of alumina: study of parameters, formal sintering analysis and hypotheses on the mechanism (s) involved in densification and grain growth, *Acta Mater.* (2011) 1400–1408.